Amino Acids (2010) 39:539–548
DOI 10.1007/s00726-009-0470-1

ORIGINAL ARTICLE

In position 7 L- and D-Tic-substituted oxytocin and deamino oxytocin: NMR study and conformational insights

Zinovia Spyranti · Maria Fragiadaki · Vassiliki Magafa · Lenka Borovickova · Georgios A. Spyroulias · Paul Cordopatis · Jirina Slaninova

Received: 28 August 2009 / Accepted: 29 December 2009 / Published online: 27 January 2010

Abstract Incorporation of L- or D-Tic into position 7 of oxytocin (OT) and its deamino analogue ([Mpa^1]OT) resulted in four analogues, [L-Tic^7]OT (**1**), [D-Tic^7]OT (**2**), [Mpa^1,L-Tic^7]OT (**3**) and [Mpa^1,D-Tic^7]OT (**4**). Their biological properties were described by Fragiadaki et al. (Eur J Med Chem 42:799–806, 2007). Their NMR study (NOESY, TOCSY, ^{1}H–^{13}C HSQC spectra) is presented here. Analogues 1, 3 and 4 showed partial agonistic activity, analogue 2 was pure antagonist, suggesting that a *cis* conformation between residues 6 and 7 of the molecule does not result in antagonistic activity. However, the reduction in agonistic activity of analogues 1, 3 and 4 in comparison to oxytocin is consistent with the reduction of the *trans* conformation form. Binding affinity for the human oxytocin receptor with IC_{50} value of 130, 730, 103, and 380 nM for peptides 1, 2, 3, and 4, respectively, showed lower affinity in the case of D analogues. Deamination slightly increased the affinity. The existence of both *cis* and *trans* configurations of the Cys^6-D-Tic^7 bond is supported by observation of two sets of cross-peaks for ^{1}H and ^{13}C nuclei for most of the residues of the peptide not only in NOESY and TOCSY but also in ^{1}H–^{13}C HSQC spectra. The MS and HPLC indicate the presence of a single molecule/peptide, and NMR data thus suggest that this second set of peaks is due to the *cis* conformation.

Keywords Oxytocin analogues · Deaminooxytocin, 1,2,3,4-tetrahydroisoquinoline-3-carboxylic acid (Tic) · NMR · Conformation

Abbreviations of common amino acids are in accordance with the recommendations of IUPAC-IUB Joint Commission on Biochemical Nomenclature: Arch Biochem Biophys 206 (1988) v–xxii, J Biol Chem 264 (1989) 668–673 and J Peptide Sci 12 (2006) 1–8.

Electronic supplementary material The online version of this article (doi:10.1007/s00726-009-0470-1) contains supplementary material, which is available to authorized users.

Z. Spyranti · M. Fragiadaki · V. Magafa · G. A. Spyroulias · P. Cordopatis
Department of Pharmacy, University of Patras, 26500 Patras, Greece

L. Borovickova · J. Slaninova
Department of Antimicrobial Peptides, Institute of Organic Chemistry and Biochemistry, Academy of Sciences of Czech Republic, Flemingovo square 2, 16610 Prague 6, Czech Republic

G. A. Spyroulias (✉)
Department of Pharmacy, University of Patras, Panepistimioupoli-Rion, 26504 Patras, Greece
e-mail: g.a.spyroulias@upatras.gr

Abbreviations

OT	Oxytocin
Mpa	β-Mercaptopropionic acid
[Mpa^1]OT, dOT	Deamino-oxytocin
Tic	1,2,3,4-Tetrahydroisoquinoline-3-carboxylic acid
Fmoc	9-Fluorenylmethoxycarbonyl
Bu^t	*t*-Butyl
Trt	Trityl
DIC	Diisopropylcarbodiimide
HOBt	1-Hydroxybenzotriazole
DMF	Dimethylformamide
DMSO	Dimethylsulfoxide
TFA	Trifluoroacetic acid
HPLC	High-performance liquid chromatography
ESI-MS	Electrospray ionization-Mass spectrometry

Introduction

The neurohypophyseal peptide hormone oxytocin (OT) is a cyclic nonapeptide with a disulfide linkage between two cysteine residues at positions 1 and 6. The N-terminal amino group is free, the C-terminus tail with the sequence Pro-Leu-Gly is amidated. Its highly potent deamino analogue (dOT) differs only in the absence of the N-terminal amino group. Among other methods, NMR was frequently used for the study of conformation of OT, dOT, vasopressin and several of their analogues (Hruby and Lebl 1987; Lebl et al. 1990; Marik et al. 2001; Budesinsky et al. 2005; Budesínsky et al. 2005; Sikorska et al. 2006; Rodziewicz-Motowidlo et al. 2008; Li et al. 2008; Zhou and Troy 2005; Zhou and Troy 2003).

First results of ^{1}H- and ^{13}C-NMR experiments with OT and arginine vasopressin (AVP) led to the consideration that the Cys^{6}-Pro^{7} bond of OT and AVP exists exclusively in the *trans* conformation (Hruby and Lebl 1987). Later, 10% *cis* isomer population in water was detected when studying the amide isomer equilibrium of the Cys^{6}-Pro^{7} bond in OT by one- and two-dimensional NMR spectroscopy (Larive et al. 1992). The relative quantity of the *cis* isomer was decreased when the solvent was changed from water to methanol (Larive and Rabenstein 1993) which agreed with the expectation that the rate of *cis*/*trans* interconversion may be faster in non-aqueous solvents (Harrison and Stein 1992). *Cis* peptide bonds were latter also observed in sarcosyl^{7}-, *N*-methylalanyl^{7}-, thiazolidine-4-carboxylic acid^{7} or 3,4-didehydroproline^{7}-OT analogues (Grzonka et al. 1985; Grzonka et al. 1983; Rodziewicz-Motowidlo et al. 2002; Rosamond and Ferger 1976; Moore et al. 1977). Introduction of glycine into position 7 leads to a decrease of uterotonic activity though to an increase of selectivity (Hruby and Lebl 1987; Lowbridge et al. 1977). All the results indicate that proline in position 7 is an important conformational constraint necessary for biological activity.

Structure–activity studies concerning the structural features leading to agonism or antagonism of oxytocin effect on uterus prompted investigations on the hypothesis that antagonism is due to the *cis* Cys^{6}-Pro^{7} isomer, whereas the *trans* isomer results in agonistic activity. For example, the *cis* Cys-Pro peptide bond was observed in the potent bicyclic antagonists of OT, [Mpa^{1},cyclo(Glu^{4},Lys^{8})]OT and [dPen^{1},cyclo(Glu^{4},Lys^{8})]OT, by NMR spectroscopy and computational analysis (Shenderovich et al. 1997). The X-ray structure of the potent OT agonist, [Mpa^{1}]OT (dOT), showed the Cys-Pro imide bond in the *trans* conformation (Wood et al. 1986). These observations led Lubell and others to synthesize analogues of OT, [Mpa^{1}]OT, and [dPen^{1}]OT having replaced Pro^{7} by (2S,5R)-5-*tert*-butylproline, a proline analogue inducing up to 90% of the *cis* amide conformation in *N*-(acetyl)dipeptide-*N*′-methylamides as shown previously (Belec et al. 2000; Bélec et al. 2001).

Wittelsberger et al. (2005) on the other hand reported the synthesis and the conformational and biological properties of thiazolidine and oxazolidine derivatives in position 7 that served as proline analogues with increased proline-specific properties. The dimethyl-substituted derivatives, 2,2-dimethyl-1,3-thiazolidine-4-carboxylic acid and 2,2-dimethyl-1,3-oxazolidine-4-carboxylic acid, induce up to 95% of the *cis* conformation as determined by one- and two-dimensional NMR spectroscopy in DMSO and in water. The impact of the dimethyl moiety at 2-C was assessed by comparison with the corresponding dihydro compound, [Cys($\varphi^{H,H}$pro)]^{7}OT. Comparison of the oxytocic activities of the *cis*-constrained compounds and OT showed that the agonistic potency increased proportionally to the *trans* content of the 6-7 peptide bond; however, no antagonistic activity was observed for the *cis*-constrained analogue, weakening the possibility that the *cis* conformation is necessary for antagonism. The results lead however to the hypothesis that the *cis*/*trans* conformational change is playing a role in OT receptor binding and activation. There was one interesting finding and thus that in the absence and presence of magnesium ions, a considerable change was observed in the pattern of the HR protons of residues 3 and 1, indicating conformational changes that influence activity (Wittelsberger et al. 2005). Also in the case of cyclic analogues, the structural analysis revealed β-turns around residues Tyr^{2} and Ile^{3}, which differed from the previously discussed β-turn geometry around residues 3 and 4 that was ascribed to the conformation of OT agonists (Hruby and Lebl 1987; Oldziej et al. 1995).

Recently we have published the synthesis and biological activities of four new OT and dOT analogues having incorporated L- or D-1,2,3,4,-tetrahydroisoquinoline-3-carboxylic acid (L- or D-Tic) into position 7 (Fragiadaki et al. 2007), i.e., [L-Tic^{7}]OT (**1**), [D-Tic^{7}]OT (**2**), [Mpa^{1}, L-Tic^{7}]OT (**3**) and [Mpa^{1},D-Tic^{7}]OT (**4**). As their biological activities have been very interesting (see Table 1) we decided to study their structure more deeply. The NMR study (determination and analysis of NOESY, TOCSY, and ^{1}H–^{13}C HSQC spectra) is presented in this paper.

Materials and methods

NMR spectroscopy

Data were acquired at 298 K on a Bruker Avance 600 MHz spectrometer. ^{1}H 1D NMR spectra were recorded using spectral width of 12–17 ppm with or without presaturation

Table 1 Biological activities of studied oxytocin analogues

	Analogues	Biological activity			
		Uterotonic in vitro		Pressor	
		Agonistic (IU/mg)	Antagonistic (pA_2)	Agonistic[a] (IU/mg)	Antagonistic (pA_2)
	Oxytocin	546		5	
1	[L-Tic^7]OT	~2.00	~5.60	0	0[b]
2	[D-Tic^7]OT	0	7.00 ± 0.30	0	0[b]
	[Mpa^1]OT(deamino-oxytocin)	803		1.4	0
3	[Mpa^1,L-Tic^7]OT	~3.50	7.45 ± 0.28	0	0[b]
4	[Mpa^1,D-Tic^7]OT	~1.00	8.00 ± 0.10	0	0

From ref. Bélec et al. (2001)

[a] 0 means no activity up to the dose 0.16 mg/kg of exp. animal

[b] Means no activity or very low inhibitory activity $pA_2 < 6$

of the H_2O signal. ^1H–^1H 2D TOCSY (Braunschweiler and Ernst 1983; Bax and Davis 1985) were recorded using the MLEV-17 spin lock sequence using $\tau_m = 80$ ms, and ^1H–^{13}C HSQC (Bax and Grzesiek 1993; Bothner-By et al. 1984) with 200.791 ppm spectral width in F1. ^1H–^1H TPPI NOESY (Marion and Wüthrich 1983; Jeener et al. 1979) spectra were acquired using mixing time $\tau_m = 300$ ms applying water suppression during the relaxation delay and mixing time. All 2D spectra were acquired with 10.014 ppm spectral width, consisting of 2 K data points in the F2 dimension, 16–32 transients and 512–1,024 complex increments in the F1 dimension. Raw data were multiplied in both dimensions by a pure cosine-squared bell window function and Fourier-transformed to obtain 2,048 × 2,048 real data points. A polynomial base-line correction was applied in both directions. For data processing and spectral analysis, the standard Bruker software (XWinNMR 3.5) and XEASY (Eccles et al. 1991) program (ETH, Zurich) were used.

NOE constraints

313, 286, 225 and 440 NOESY cross-peaks were assigned in both dimensions for [D-Tic^7]OT, [Mpa^1,D-Tic^7]OT, [Mpa^1,L-Tic^7]OT and [L-Tic^7]OT, respectively, in DMSO. The number of unique cross-peaks were 151, 136, 124 and 216 (15, 14, 13 and 22 constraints per residue for [D-Tic^7]OT, [Mpa^1,D-Tic^7]OT, [Mpa^1,L-Tic^7]OT and [L-Tic^7]OT, respectively). Their intensities were converted into upper limit distances through CALIBA (Güntert et al. 1991). Sequential constraints, number and range of NOEs and chemical shift differences ($\{(\Delta\delta_{H\alpha})^2 + (\Delta\delta_{HN})^2\}^{1/2}$) are illustrated in Online Resources 1, 2 and 3.

Structure calculations and refinement

The NOE-derived structural information extracted from the analysis of NOESY spectra acquired in DMSO $-d_6$ solutions under identical experimental conditions for all three peptides was introduced to DYANA (Güntert et al. 1997; Wüthrich et al. 1983) software for structure calculations. The peptide models in the figures have been generated with MOLMOL (Pearlman et al. 1997). Structural calculations have been performed on IBM RISC6000 and xw4100/xw4200 HP Linux workstations. 3J(NH–Hα) coupling constants were determined by inverse Fourier transformation of in-phase multiplets from NOESY spectra using the INFIT routine of the XEASY software (Eccles et al. 1991).

Results

Proton assignment

TOCSY maps were first analyzed to assign the individual spin patterns of amino acids through scalar connectivities. Sequential, medium and long range connectivities were identified from NOESY maps acquired with $\tau_m = 300$ ms. Chemical shifts for the four peptides are reported in Tables 2, 3, 4, and 5. Characteristics TOCSY fingerprints regions are given in Fig. 1.

*[L-Tic^7]OT (**1**)*

The NOE pattern involving HN–HN, Hα–HN and Hβ–HN (i, $i + 1$) connectivities for this peptide is rather similar to the [Mpa^1,L-Tic^7]OT peptide (Online Resource 2). The

Table 2 Chemical shifts (in ppm) and 3J(NH–Hα) coupling constants (in Hz) of the residues in the [D-Tic^7]OT peptide at 298 K (DMSO-d_6)

	Residue	HN	Hα	Hβ	Other	3J (NH,Hα)
1	Cys	8.069	4.959	3.139, 3.041	–	3.4
2	Tyr	8.011	4.581	3.126, 2.737	Hδ 7.095; Hε 6.663	7.4
3	Ile	8.068	4.100	1.506	Hγ 1.442; γCH$_3$ 0.822; δCH$_3$ 0.708	3.5
4	Gln	8.173	4.007	1.888, 1.825	Hγ 2.143; δCH$_3$ 7.316, 6.807	6.6
5	Asn	8.033	4.448	2.654, 2.593	δNH$_2$ 6.911, 7.405	8.9
6	Cys	8.714	4.437	3.260; 3.022	–	7.7
7	DTic	–	3.912	1.844, 0.873	Hγ 1.482, 1.158	–
8	Leu	7.734	4.106	1.498	Hγ 1.442; δCH$_3$ 0.819, 0.709	8.8
9	Gly	7.886	3.585, 3.502	–	–	8.0
	NH$_2$	7.156, 7.041	–	–	–	

Table 3 Chemical shifts (in ppm) and 3J(NH–Hα) coupling constants (in Hz) of the residues in the [Mpa^1,D-Tic^7]OT peptide at 298 K (DMSO-d_6)

	Residue	HN	Hα	Hβ	Other	3J (NH,Hα)
1	Mpa	–	2.956	2.403	–	–
2	Tyr	7.853	4.664	3.202, 2.631	Hδ 7.094; Hε 6.681	7.0
3	Ile	7.970	3.954	1.783	Hγ 1.554; γCH$_3$ 1.165; δCH$_3$ 0.916	3.3
4	Gln	8.401	3.907	2.028, 1.909	Hγ 2.135; δCH$_3$ 7.287, 6.802	6.5
5	Asn	7.708	4.447	2.615	δNH$_2$ 6.898, 7.464	5.7
6	Cys	8.802	4.998	3.370; 2.949	–	6.4
7	DTic	–	3.863	1.807, 0.897	Hγ 1.549, 1.171; Hε 7.160	–
8	Leu	8.008	4.105	1.486	Hγ 1.447; δCH$_3$ 0.823, 0.710	8.2
9	Gly	7.728	3.597, 3.526	–	–	7.9
	NH$_2$	7.142, 7.027	–	–	–	

Table 4 Chemical shifts (in ppm) and 3J(NH–Hα) coupling constants (in Hz) of the residues in the [Mpa^1,L-Tic^7]OT peptide at 298 K (DMSO-d_6)

	Residue	HN	Hα	Hβ	Other	3J (NH,Hα)
1	Mpa	–	2.927	2.423	–	–
2	Tyr	7.845	4.667	3.257, 2.642	Hδ 7.147; Hε 6.693	7.0
3	Ile	8.377	3.805	1.791	Hγ 1.576;.γCH$_3$ 1.196; δCH$_3$ 0.912	3.4
4	Gln	8.326	3.884	2.013, 1.864	Hγ 2.124; δCH$_3$ 6.802, 7.287	6.2
5	Asn	7.687	4.542	2.610, 2.573	δNH$_2$ 6.900, 7.387	7.9
6	Cys	8.766	5.195	3.332; 2.934	–	7.8
7	LTic	–	3.997	1.545, 0.645	Hγ 1.400, 0.780; Hε 7.222	–
8	Leu	7.475	4.086	1.320	Hγ 1.238; δCH$_3$ 0.621, 0.554	7.9
9	Gly	7.367	3.641, 3.453	–	–	7.9
	NH$_2$	7.188, 7.078	–	–	–	

Hα–HN and Hβ–HN (i, $i + 2$) NOEs network involves residues Tyr^2 and Gln^4. Moreover, Hα–HN and Hβ–HN of (i, $i + 3$) type connectivities are also identified between Tyr^2 and Asn^5. This finding is also supported by the formation of a (i, $i + 3$) hydrogen bond between residues Tyr^2 and Asn^5 observed in all 20 calculated models. The observed NOEs between Cys^1 and Cys^6 suggest that these residues are in close proximity in a similar way as in the other studied peptides. Among the noteworthy NOEs are those of the medium-range connectivities between Tyr^2-L-Tic^7,

Table 5 Chemical shifts (in ppm) and 3J(NH–Hα) coupling constants (in Hz) of the residues in the [L-Tic^7]OT peptide at 298 K (DMSO-d_6)

	Residue	HN	Hα	Hβ	Other	3J (NH,Hα)
1	Cys	8.306	5.254	3.180; 3.075	–	3.4
2	Tyr	8.501	4.670	3.339, 2.754	Hδ 7.168; Hε 6.706	7.3
3	Ile	8.078	4.036	1.511	Hγ 1.367; γCH$_3$ 1.119; δCH$_3$ 0.547	–[a]
4	Gln	8.422	3.868	1.840, 1.783	Hγ 2.172; δCH$_3$ 6.852, 7.352	6.5
5	Asn	7.531	4.618	2.663, 2.604	δNH$_2$ 7.070, 7.450	8.9
6	Cys	8.770	4.557	3.066; 2.761	–	8.7
7	LTic	–	3.742	1.848, 0.912	Hγ 1.201, 1.529; Hε 7.224	–
8	Leu	7.390	4.061	1.320	Hγ 1.181; δCH$_3$ 0.502, 0.609	6.9
9	Gly	7.904	3.628, 3.533	–	–	−8.3
	NH$_2$	7.135, 7.040	–	–		

[a] Due to excessive overlap, the coupling constant could not be measured

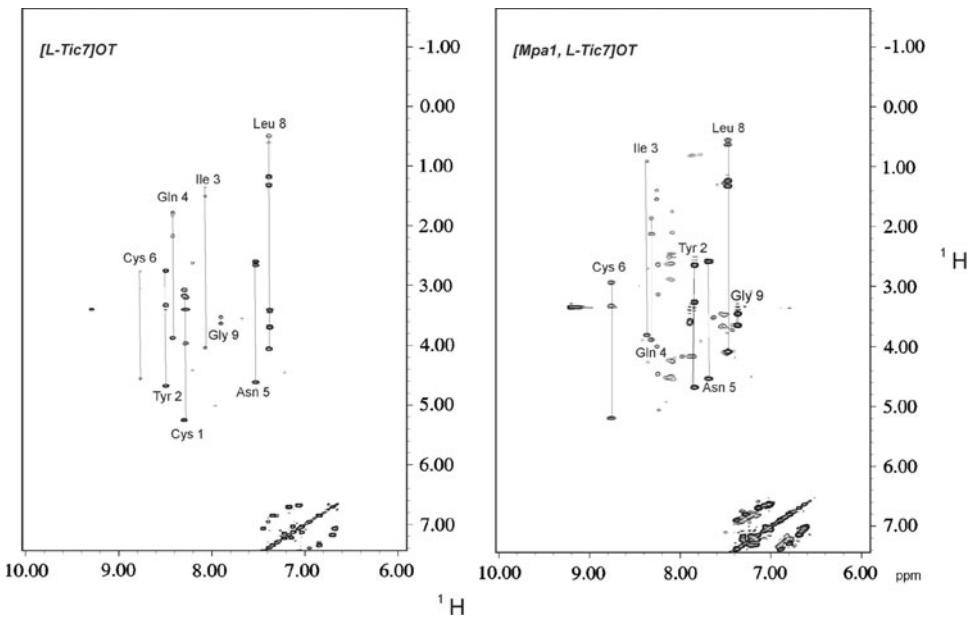

Fig. 1 Characteristic TOCSY fingerprints regions of [L-Tic^7]OT (*left*) and [Mpa^1,L-Tic^7]OT (*right*) extracted from 2D ^{1}H 600-MHz NMR recorded in DMSO–d_6 at 298 K

which are not detected in NOESY spectra of the other three peptides, [D-Tic^7]OT, the [Mpa^1,D-Tic^7]OT and [Mpa^1, L-Tic^7]OT.

*[D-Tic^7]OT (**2**)*

Numerous HN–HN, Hα–HN and Hβ–HN sequential connectivities are detected in the region Cys^1-L-Tic^7 and Leu^8-NH$_2^{10}$, while Hα–HN and Hβ–HN of (i, $i + 2$) type connectivities between Cys^6 and Leu^8 have also been observed. Furthermore, (i, $i + 2$) type connectivities have been identified between the Hα and Hβ proton of Cys^1 with Hα and Hδ proton of Ile^3. The medium-range connectivities between the Hβ proton of Cys^1 and the amide proton of Asn^5 are among the characteristic NOEs that indicate the spatial proximity of these amino acids. Schematic representation of the sequential and medium range connectivities is given in Online Resource 1.

*[Mpa^1,L-Tic^7]OT (**3**)*

Numerous HN–HN sequential connectivities are detected in the region Mpa^1-Ile^3 and Gln^4-L-Tic^7 and Leu^8-NH$_2^{10}$, while Hα–HN and Hβ–HN sequential connectivities are also identified between all residues, except L-Tic^7. Furthermore, an HN–HN of (i, $i + 2$) connectivity between Ile^3-Asn^5 has also been observed. A Hα–HN of (i, $i + 2$) type connectivity between Cys^6-Leu^8 has also been identified. The medium-range connectivities between the Mpa^1 Hβ proton and the Hα proton of Cys^6 are among the characteristic NOEs further supporting the spatial proximity of these residues. Schematic representation of the

sequential and medium range connectivities is given in Online Resource 2.

*[Mpa^1,D-Tic^7]OT (**4**)*

The NOE pattern involving HN–HN, Hα–HN and Hβ–HN (i, $i + 1$) connectivities for this peptide is rather similar to the [D-Tic^7]OT peptide. HN–HN and Hα–HN (i, $i + 2$) type connectivities are observed for the tripeptide comprised of Tyr^2-Ile^3-Gln^4, while Hβ–HN (i, $i + 2$) type NOEs are also identified among residues Tyr^2-Ile^3-Gln^4, Ile^3-Gln^4-Asn^5 and Cys^6-Pro^7-Leu^8. The observed NOE network in concern with HN-HN connectivity between Ile^3-Cys^6 suggests a turn-like structure comprised of these residues. Additionally, two medium-range NOEs of Hβ protons of Mpa^1 with Hα and Hβ protons of Cys^6 indicate that these residues of the peptide are in close proximity in a similar way as in [D-Tic^7]OT peptide. Furthermore, the formation of a hydrogen bond between residues Ile^3 and Asn^5 is consistent in all 20 calculated models. Schematic representation of the sequential and medium range connectivities is given in Online Resource 1.

Chemical shift difference analysis

Two diagrams illustrating the ^{1}H chemical shift differences between the peptide pairs were plotted. The variations in chemical shifts are potential indicators for the conformational changes imposed by the replacement of the amino acids at position 7 (Online Resource 3). These plots refer to the peptide pairs [D-Tic^7]OT-[Mpa^1,D-Tic^7]OT and [L-Tic^7]OT-[Mpa^1,L-Tic^7]OT. The largest chemical shift variation in the first peptide pair [D-Tic^7]OT-[Mpa^1, D-Tic^7]OT (black) was observed for Cys^6 (>0.40 ppm), while smaller variations were calculated for Asn^5 and Leu^8, suggesting conformational rearrangements between the two peptides. The introduction of Mpa^1 in position 1, which is a non-protein residue and is less bulky than Cys^1, has been shown to affect the chemical environment and consequently the nature of the disulfide bond linking positions 1 and 6. Furthermore, Asn^5, which lies in the middle of the sequence, seems to be affected by modification in position 1.

In the other peptide pair [L-Tic^7]OT-[Mpa^1,L-Tic^7]OT the largest chemical shift variations are calculated for Tyr^2 and Cys^6 (>0.60 ppm) affected by modification in position 1. A smaller variation is observed for Gly^9 (>0.50 ppm), suggesting a different conformation for the tripeptide segment Pro^7-Leu^8-GlyNH$_2^9$.

Another two diagrams illustrating the ^{1}H chemical shift differences were plotted for peptide pairs [Mpa^1, D-Tic^7]OT-[Mpa^1,L-Tic^7]OT and [D-Tic^7]OT-[L-Tic^7]OT (Online Resource 3). As far as the [Mpa^1,D-Tic^7]OT-[Mpa^1,L-Tic^7]OT peptide pair is concerned, the largest chemical shift variation was observed for Leu^8 (>0.50 ppm), while smaller variations were calculated for Ile^3 and Gly^9 (>0.30 ppm) suggesting conformational rearrangements between the two peptides (Online Resource 3). The chemical shift variation of Ile^3 is justified by the NOE network involving amino acids Ile^{3}and Cys^6, present only in the [Mpa^1,D-Tic^7]OT peptide. As a conclusion, the modification in position 7 suggests small conformational rearrangements of the fragment Leu^8-GlyNH$_2^9$ between the two peptides.

As far as the [D-Tic^7]OT-[L-Tic^7]OT peptide pair is concerned, the largest chemical shift variation was observed for Asn^5 (>0.50 ppm), while smaller variations were calculated for Tyr^2 and Leu^8 (>0.30 ppm) suggesting conformational rearrangements between the two peptides. The chemical shift variations of Asn^5 and Tyr^2 are justified by the NOE network involving amino acids Cys^1-Asn^5 in the [D-Tic^7]OT peptide, and by NOEs between Tyr^2-L-Tic^7, present only in the [L-Tic^7]OT peptide. The chemical shift variation calculated for Leu^8 (>0.30 ppm) is justified by the modification of the amino acid in position 7.

Structure calculations and conformational analysis

The average target function for the DYANA family of 20 calculated models was found to be $0.32 \pm 1.34 \times 10^{-5}$ Å^2 for [D-Tic^7]OT, 0.11 ± 0.003 Å^2 for [Mpa^1,D-Tic^7]OT, $0.66 \pm 1.06 \times 10^{-7}$ Å^2 for [Mpa^1,L-Tic^7]OT and 0.45 ± 0.23 Å^2 for [L-Tic^7]OT peptide models. No consistent violations existed at the final DYANA run and no constrained violation was found larger than 0.30 Å.

The DYANA family models for [D-Tic^7]OT peptide exhibit pairwise rmsd values for all residues 0.10 ± 0.05 Å (BB), 1.26 ± 0.48 Å (HA) for the 20 structures. The rmsd values for [Mpa^1,D-Tic^7]OT ensemble are 0.36 ± 0.43 Å (BB), 0.99 ± 0.61 Å (HA) for the 20 models, while for [Mpa^1,L-Tic^7]OT are found 1.00 ± 0.44 Å (BB), 2.50 ± 0.73 Å (HA) for the 20 models. Furthermore, the DYANA family models for [L-Tic^7]OT peptide exhibit rmsd values for all residues 0.69 ± 0.48 Å (BB), 1.62 ± 0.52 Å (HA) for the 20 structures.

3D solution structures

The NMR data for the four analogues indicate that the residue in position 1 (Cys^1/Mpa^1) remains in close spatial proximity with Cys^6. Medium range NOEs between residues Cys^1/Mpa^1 and Cys^6 are fully consistent with the fact that Cys^1/Mpa^1 and Cys^6 are linked through a disulfide bond. In general, [D-Tic^7]OT, [Mpa^1,D-Tic^7]OT and [Mpa^1,L-Tic^7]OT peptides exhibit a lower number of NOE cross-peaks (151, 136 and 124 cross-peaks, respectively) relative to the [L-Tic^7]OT peptide (216 NOE cross-peaks).

Highly populated hydrogen bonds are identified through the analysis of the NMR solution models ensemble. Specifically, both analogues bearing LTic in position 7 of the peptide sequence form a hydrogen bond involving amino acids in positions 2 and 5. In the [LTic^7]OT analogue, a strong backbone hydrogen bond is identified between Tyr^2-NH and the Asn^5-CO (1.42–1.55 Å). Additionally, a diagnostic tool for the determination of a turn structure is the C_α distance of the residues (Lewis et al. 1973). To this context, the C_α atoms of Tyr^2 and Asn^5 are found in close proximity (4.37–5.00 Å). In the [Mpa^1,LTic^7]OT analogue, a high populated H-bond is formed between the amide proton of Asn^5 and the carbonyl oxygen of Tyr^2 (1.57–2.09 Å), while the distance between the C_α atoms of these amino residues is measured 4.40–4.49 Å. The above data suggest regular β-turns for both [LTic^7]OT and [Mpa^1, LTic^7]OT peptides comprised of Tyr^2-Asn^5 residues. Applying the same criteria as above, for the [Mpa^1,DTic^7]OT analogue, the turn formed bears the conformational features of a γ-turn. A very highly populated hydrogen bong, observed in 19 out of the 20 calculated structures of the ensemble, is formed among residues Asn^5-NH and Ile^3-CO (1.87–2.32 Å) in the [Mpa^1,DTic^7]OT analogue. The distance between the C_α atoms of Tyr^2 and Asn^5 is found to be 2.4–3.4 Å. Moreover, a second weaker H bond is identified between Hδ protons of Asn^5 and the carbonyl oxygen of Gln^4, present in 10 out of 20 calculated structures. Concerning the [DTic^7]OT peptide, no highly populated hydrogen bonding is identified and no safe conclusion can be extracted from the analysis of the NMR data and calculated models for the assignment of this turn conformation to any of β- or γ-turns.

In the [L-Tic^7]OT analogue, residues Cys^1 and Cys^6 are also found to be in close proximity as manifested by medium-range NOEs, such as the Hβ proton of Cys^1 with the amide proton of Cys^6, as well as the amide proton of Tyr^2 with the amide proton of Asn^5 and Cys^6. The observed NOEs are indicative for a local conformation that favours the formation of a hydrogen bond between Tyr^2 and Asn^5 observed in the family of 20 best DYANA structures, while a turn is formed by residues Ile^3-Gln^4-Asn^5. Furthermore, the Hα–HN of (i, $i + 2$) and Hβ–HN of (i, $i + 2$) type NOE connectivities for residues Tyr^2 and Gln^4 indicate the formation of a type II-β turn for this segment. Moreover, (i, $i + 3$) type connectivities between Tyr^2 and Asn^5 further support the backbone turn for this region (Fig. 2).

According to the NMR analysis and structure calculations presented here, [L-Tic^7]OT shares some similar conformational features with [Mpa^1,L-Tic^7]OT. Residues Mpa^1 and Cys^6 are also found in spatial proximity. The vicinity of these residues is supported by a significantly smaller amount of NOEs than in the case of the [L-Tic^7]OT peptide, which leads to a less compact structure (Fig. 3).

A backbone turn involving residues Ile^3-Gln^4-Asn^5 is observed in the [Mpa^1,L-Tic^7]OT peptide, supported by (i, $i + 2$) type connectivities between residues Ile^3-Asn^5, similar to the [L-Tic^7]OT analogue. In contrast, their side chains are oriented to opposite directions, possibly due to the observed NOEs between amino acids Cys^6-Leu^8, present only in the [Mpa^1,L-Tic^7]OT peptide (Fig. 3).

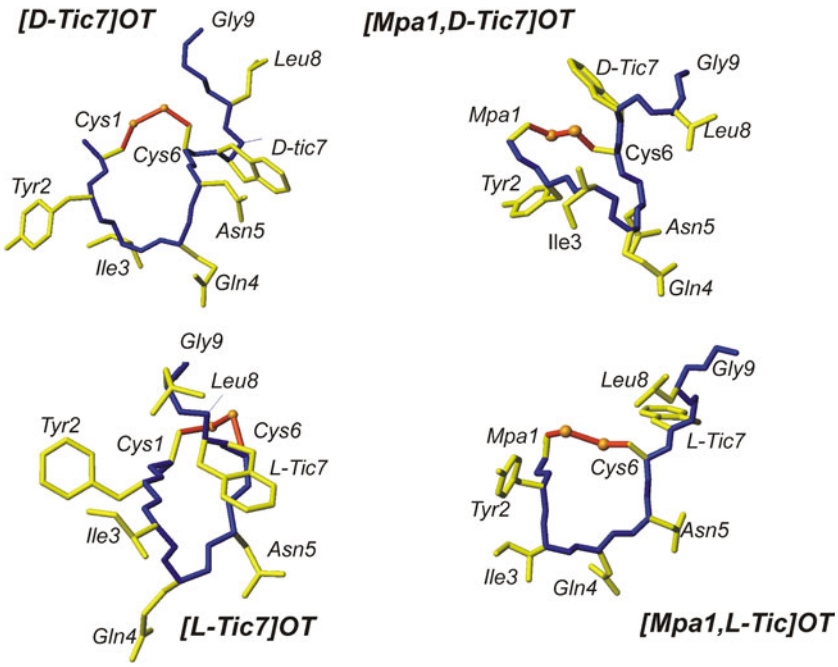

Fig. 2 Mean structures calculated for the [D-Tic^7]OT, [Mpa^1,L-Tic^7]OT, [L-Tic^7]OT and [Mpa^1,D-Tic^7]OT analogues. Figures were generated with the MOLMOL program

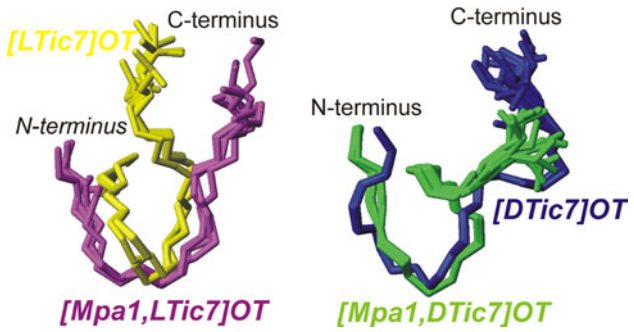

Fig. 3 Superimposition of the backbone of the two peptide pairs; [L-Tic7]OT-[Mpa^1,L-Tic^7]OT (*left*) as well as [D-Tic^7]OT-[Mpa1, D-Tic7]OT (*right*). Figures are generated with MOLMOL

The NMR data for [D-Tic^7]OT and [Mpa^1,D-Tic^7]OT peptides indicate that residues in positions 1 and 7 are in close spatial proximity (Fig. 3). Medium-range NOEs between Cys^1 and Asn^5 present in the [D-Tic^7]OT peptide and NOEs between Mpa^1 and Cys^6 in the [Mpa^1,D-Tic^7]OT peptide support the vicinity of these peptide residues. The formation of a hydrogen bond between Ile^3-Asn^5 observed in all 20 calculated models of [Mpa^1,D-Tic^7]OT peptide further supports this finding. The overall conformation of the backbone for the segment Cys^1/Mpa^1-Cys^6 reveals great structural similarities between the two analogues, but also some differences. NOE (i, $i + 2$) connectivities between Cys^1 and Ile^3 indicate the formation of a backbone bend for this segment in the [D-Tic^7]OT peptide. On the other hand, NOE interactions between (1) Hβ protons of Tyr^2 with the amide proton of Gln^4 and (2) the amide proton of Ile^3 with the amide proton of Asn^5 and Cys^6 lead the [Mpa^1,D-Tic^7]OT peptide to adopt a turn-like structure comprised of these residues.

As far as the fragment of Cys^6-D-Tic^7-Leu^8-Gly^{9}NH$_2$ is concerned; both OT peptides exhibit a backbone turn due to the (i, $i + 2$) type connectivities of Hβ proton of Cys^6 with the amide proton of Leu^8, observed in both peptides. However, NOE connectivities of Hβ proton of Cys^6 with the Hβ and the side chain protons of Leu^8, present only in the [D-Tic^7]OT peptide, lead the two amino residues to adopt a parallel orientation in space with the side chain protons of Leu^8 lying in the same region in space with Hβ protons of Cys^6. The segment comprised of Leu^8-Gly^{9}NH$_2$ exhibits a rather extended backbone conformation for both [D-Tic^7]OT and [Mpa^1,D-Tic^7]OT peptides.

As a conclusion, deamination in position 1 influences the conformational flexibility of Cys^1/Mpa^1–Cys^6, which in turn affects the geometry of the disulfide bond and imposes a conformational difference among the peptides. On the other hand, the change of configuration of amino acid in position 7 (replacement of L-Tic^7 by D-Tic^7) is inducing smaller conformational changes in the backbone of the OT peptides in the case of deamino analogues than the amino analogues (Fig. 3). The N-terminal 7-residue fragment of the [Mpa^1,L-Tic^7]OT and [Mpa^1,D-Tic^7]OT peptides adopts the very same backbone conformation (Fig. 3). The backbone structure of the 3-residue fragment of the C-terminus is also similar among the peptides with the different orientation, resulting from replacement of L-Tic^7 by D-Tic^7, being the main difference among the [Mpa^1,L-Tic^7]OT and [Mpa^1,D-Tic^7]OT peptides. Finally, it is worth noting that the distribution of the amino acids in the tertiary structures leads the peptides to form a polar face and a more polar side. Tyr^2, Gln^4 and Asn^5 lead the peptide to adopt a solvent exposed polar face, while the hydrophobic aminoacids Tic^7 and Leu^8 form the C-terminal tripetide.

Discussion

Literature data indicate that the neurohypophyseal hormone analogues lacking the N-terminal amino group are inactivated slower than the mother compounds and have enhanced biological activities both agonistic and antagonistic ones (Oldziej et al. 1995; Fragiadaki et al. 2007). The anti-oxytocic activity was significantly enhanced in the case of both analogues [Mpa^1,L-Tic^7]OT and [Mpa^1,D-Tic^7]OT, while the agonistic activity was only slightly affected (Bélec et al. 2001). Furthermore, the first amino acid seems to play a decisive role in receptor binding (Oldziej et al. 1995; Fragiadaki et al. 2007). In our case, deamination slightly increased the affinity of the analogues to human oxytocin receptor. It has been known that the proper orientation and the sequence of the C-terminal tripeptide are critical for obtaining high-potency OT analogues (Wittelsberger et al. 2005; Oldziej et al. 1995; Fragiadaki et al. 2007; Flouret et al. 2006). Moreover, the side chains of Ile^3 and Pro^7 are involved in the recognition and binding of the hormone by the uterine receptor (Wittelsberger et al. 2005; Oldziej et al. 1995; Fragiadaki et al. 2007; Braunschweiler and Ernst 1983). Therefore, structural modifications of the side chains in the C-terminal tripeptide might lead to analogues with variable biological properties at different OT issues. The great decrease in the agonistic potency of [L-Tic^7]OT analogue as compared to the native hormone suggests that modification at position 7 by conformational restricted and bulky residue, such as L-Tic, induces such conformational changes in the peptide backbone that cause markedly different distribution of the elements necessary for the binding of agonists and intrinsic activity.

According to our structural analysis, the replacement of amino acid L-Tic^7 by the more stereo-chemically constrained D-Tic^7 seems to induce minor conformational changes in the backbone conformation, with the main

difference being the altered side chain orientation of the C-terminal 3-residue fragment of the peptides. The presence of the D-Tic aminoacid in position 7 results in a more compact structure by limiting the local conformational flexibility, inducing a bend in the backbone conformation. This structural difference is reflected in the biological properties, with the D-counterpart being a pure antagonist with higher antagonistic potency than the L-counterpart. This finding is also confirmed in the [Mpa^1,L-Tic^7]OT-[Mpa^1,D-Tic^7]OT peptide pair, with the anti-oxytocin activity being significantly enhanced in the [Mpa^1, D-Tic^7]OT peptide. It is worth noting that the main conformational difference resulting from the substitution of L-Tic^7 with D-Tic^7 in this peptide pair is observed for the backbone conformation of the Leu^8-Gly^9 NH_2 fragment. The studied analogues are also exhibiting remarkable conformational properties from the point of view of the *cis*/*trans* isomerization of the Cys^6-Tic^7 peptide bond. The orientation of this bond and its relationship to agonism and antagonism has been previously studied; however, no direct relationship was found (Shenderovich et al. 1997; Wood et al. 1986). The introduction of the non-proteinogenic and less bulky Mpa residue in position 1 is not affecting the nature of the disulfide bond linking residues in positions 1 and 6 in oxytocin. On the contrary, the introduction of the D-Tic isomer into position 7, when position 1 is occupied by Cys, alters the geometry of the Sγ and neighboring atoms of the S–S bond (Fig. 4). The rearrangement of the C-terminal 3-residue fragment can be focused on the variation of the geometry of the Cys^6-Tic^7 peptide bond. In both [D-Tic^7]OT and [Mpa^1,D-Tic^7]OT analogues, a second set of peaks for most residues of the peptide sequence has been observed in all spectra used (NOESY, TOCSY and ^{13}C-HSQC). The population of these species is ranging between 25 and 30%, suggesting the presence of *cis*-isomerization in the peptide bond between positions 6 and 7. On the other hand, in both cases where L-Tic occupies position 7 in the peptide sequence, a unique set of peaks is observed, suggesting that Cys^6-L-Tic^7 bond is found in *trans* conformation and no *cis*-isomers are present.

According to our structural investigation of the four OT analogues and bearing in mind that D-counterparts showed higher inhibitory potency than the L-counterparts, the reduction in agonistic activity is fully consistent with the reduction of the *trans* conformation form of Cys^6-Tic^7 peptide bond.

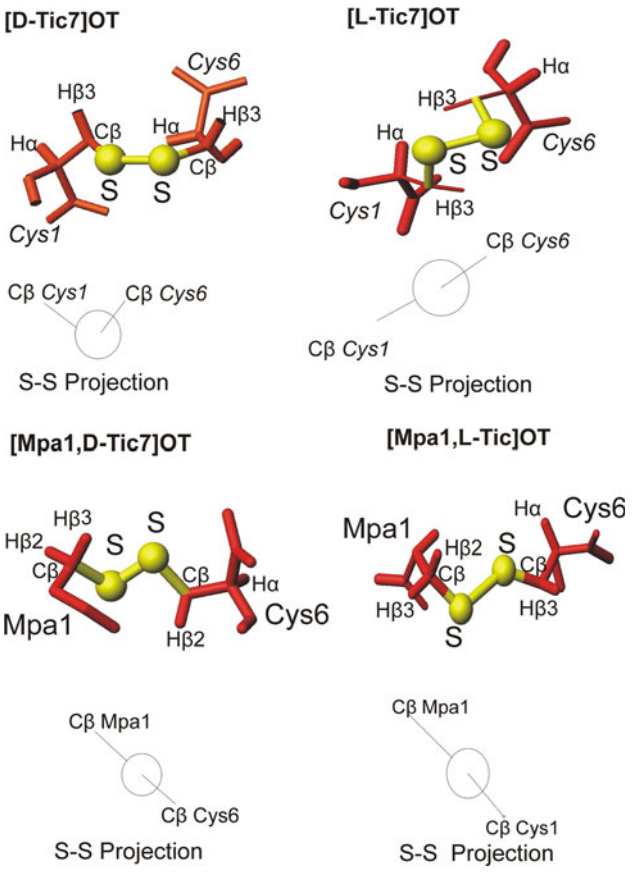

Fig. 4 Schematic representation and projection of the disulfide bond in the [D-Tic^7]OT, [L-Tic^7]OT, [Mpa^1,D-Tic^7]OT and [Mpa^1, L-Tic^7]OT analogues. Figures are generated with MOLMOL

Acknowledgments Z.S. and G.A.S. wish to acknowledge EU-NMR program—Contract # RII3-026145 (CERM; Center of Magnetic Resonance, University of Florence) for access to NMR instrumentation. The work was partly supported by research project No. Z40550506 of the IOCBof the Academy of Sciences of the Czech Republic.

References

Bax A, Davis DG (1985) MLEV-17-based two-dimensional homonuclear magnetization transfer spectroscopy. J Magn Reson 65:355–360

Bax A, Grzesiek S (1993) Methodological advances in protein NMR. Acc Chem Res 26:131–138

Belec L, Slaninova J, Lubell WD (2000) A study of the relationship between biological activity and prolyl amide isomer geometry in oxytocin using 5-*tert*-butylproline to augment the Cys6-Pro7 amide cis-isomer population. J Med Chem 43:1448–1455

Bélec L, Maletinska L, Slaninová J, Lubell WD (2001) The influence of steric interactions on the conformation and biology of oxytocin. Synthesis and analysis of penicillamine(6)-oxytocin and penicillamine(6)-5-tert-butylproline(7)-oxytocin analogs. J Pept Res 58:263–273

Bothner-By AA, Stephens RL, Lee JM, Warren CD, Jeanloz RW (1984) Structure determination of a tetrassacharide: transient nuclear overhauser effect in the rotating frame. J Am Chem Soc 106:811–813

Braunschweiler L, Ernst RR (1983) Coherence transfer by isotropic mixing: application to proton correlation spectroscopy. J Magn Reson 53:521–528

Budesinsky M, Ragnarsson U, Lankiewicz L, Grehn L, Slaninova J, Hlavacek J (2005) Synthesis and utilisation af 13C and 15N backbone-labelled proline: NMR study of synthesized oxytocin with backbone-labelled C-terminal tripeptide amid. Amino Acids 29:151–160

Budesínsky M, Procházka Z, Slaninová J (2005) Oxytocin and its analogs, methyl-substituted in ortho-, meta- or para-position of aromatic ring of phenylalanine in position 2: NMR study and biological activities. Protein Pept Lett 12:343–347

Eccles C, Güntert P, Billeter M, Wüthrich K (1991) Efficient analysis of protein 2D NMR spectra using the software package EASY. J Biomol NMR 1:111–130

Flouret G, Chaloin O, Borovickova L, Slaninova J (2006) Design of novel bicyclic analogues derived from a potent oxytocin antagonist. J Pept Sci 12:412–419

Fragiadaki M, Magafa V, Borovickova L, Slaninova J, Cordopatis P (2007) Synthesis and biological activity of oxytocin analogues containing conformationally-restricted residues in position 7. Eur J Med Chem 42:799–806

Grzonka Z, Lammek B, Kasprzykowski F, Gazis D, Schwartz IL (1983) Synthesis and some pharmacological properties of oxytocin and vasopressin analogues with sarcosine or *N*-methyl-L-alanine in position 7. J Med Chem 26:555–559

Grzonka Z, Mishra PK, Bothner-By AA (1985) Conformational preferences and binding to neurophysins of oxytocin analogues with sarcosine or *N*-methylalanine in position 7. Int J Pept Protein Res 25:375–381

Güntert P, Braun W, Wüthrich K (1991) Efficient computation of three-dimensional protein structures in solution from nuclear magnetic resonance data using the program DIANA and the supporting programs CALIBA, HABAS and GLOMSA. J Mol Biol 217:517–530

Güntert P, Mumenthaler C, Wüthrich K (1997) Torsion angle dynamics for NMR structure calculation with the new program DYANA. J Mol Biol 273:283–298

Harrison RK, Stein RL (1992) Mechanistic studies of enzymic and nonenzymic prolyl cis-trans isomerization. J Am Chem Soc 114:3464–3471

Hruby VJ, Lebl M (1987) Conformational properties of neurohypophyseal hormone analogs in solution as determined by NMR and Laser Raman Spectroscopies. In: Jost K, Lebl M, Brtnik F (eds) Handbook of neurohypophyseal hormone analogs, vol 1, part 1. CRC Press, Boca Raton, pp 105–154

Jeener J, Meier BH, Bachmann P, Ernst RR (1979) Investigation of exchange processes by two-dimensional NMR spectroscopy. J Chem Phys 71:4546–4553

Larive CK, Rabenstein DL (1993) Dynamics of cis/trans isomerization of the cysteine6-proline peptide bonds of oxytocin and arginine-vasopressin in aqueous and methanol solutions. J Am Chem Soc 115:2833–2836

Larive CK, Guerra L, Rabenstein DL (1992) Cis/trans conformational equilibrium across the cysteine6-proline peptide bond of oxytocin, arginine vasopressin, and lysine vasopressin. J Am Chem Soc 114:7331–7337

Lebl M, Hill P, Kazmierski W, Karaszova L, Slaninova J, Fric I, Hruvby VJ (1990) Conformationally restricted analogs of oxytocin; stabilization of inhibitory conformation. Int J Pept Protein Res 36:321–330

Lewis PN, Momany FA, Scheraga HA (1973) Chain reversals in proteins. Biochim Biophys Acta 303:211–229

Li X, Peterkofsky A, Wang G (2008) Solution structure of NPr, a bacterial signal-transducing protein that controls the phosphorylation state of the potassium transporter-regulating protein IIANtr. Amino Acids 35:531–539

Lowbridge J, Manning M, Haldar J, Sawyer WH (1977) Synthesis and some pharmacological properties of [4-threonine, 7-glycine]-oxytocin, [1-(L-2-hydroxy-3-mercaptopropanoic acid), 4-threonine, 7-glycine]oxytocin (hydroxy[Thr4, Gly7]oxytocin), and [7-Glycine]oxytocin, peptides with high oxytocic-antidiuretic selectivity. J Med Chem 20:120–123

Marik J, Budesinsky M, Slaninova J, Hlavacek J (2001) Synthesis, bioassay and NMR study of methyleneoxy isosters of oxytocin and vasopressin. Collect Czech Chem Commun 67:373–392

Marion D, Wüthrich K (1983) Application of phase sensitive two-dimensional correlated spectroscopy (COSY) for measurements of 1H–1H spin-spin coupling constants in proteins. Biochem Biophys Res Commun 113:967–974

Moore S, Felix AM, Meienhofer J, Smith CW, Walter R (1977) Pharmacological effects of introducing a double bond into a binding site of oxytocin. Analogues with L-3, 4-dehydroproline in position 7. J Med Chem 20:495–500

Oldziej S, Ciarkowski J, Liwo A, Shelderovich MD, Grzonka Z (1995) Conformational aspects of differences in requirements for oxytocin and vasopressin receptors. J Recept Signal Transduct Res 15:703–713

Pearlman DA, Case DA, Caldwell JW, Ross WS, Cheatham TE, Ferguson DM, Seibel GL, Singh UC, Weiner PK, Kollman PA (1997) AMBER 5.0. University of California, San Francisco

Rodziewicz-Motowidlo S, Zhukov I, Kasprzykowski F, Grzonka Z, Ciarkowski J, Wojcik J (2002) Conformational solution studies of (Sar7) desamino and (MeAla7) desaminovasopressin analogues using NMR spectroscopy. J Pept Sci 8:347–364

Rodziewicz-Motowidlo S, Sikorska E, Oleszczuk M, Czaplewski C (2008) Conformational studies of vasopressin and mesotocin using NMR scectroscopy and molecular modelling methods. II. Studies in the SDS micelle. J Pept Sci 14:85–96

Rosamond JD, Ferger MF (1976) Synthesis and some pharmacologicalproperties of oxytocin analogues having L-thiazolidine-4-carboxylic acid in position 7. J Med Chem 19:873–876

Shenderovich MD, Koever KE, Wilke S, Collins N, Hruby VJ (1997) Solution conformations of potent bicyclic antagonists of oxytocin by nuclear magnetic resonance spectroscopy and molecular dynamics simulations. J Am Chem Soc 119:5833–5846

Sikorska E, Slusarz M, Slusarz R, Kowalczyk W, Lammek B (2006) Investigation of cis/trans ratios of peptide bonds in AVP analogues. J Pept Sci 12:13–24

Wittelsberger A, Patiny L, Slaninova J, Barberis C, Mutter M (2005) Introduction of a cis-prolyl mimic in position 7 of the peptide hormone oxytocin does not result in antagonistic activity. J Med Chem 48:6553–6562

Wood SP, Tickle IJ, Treharne AM, Pitts JE, Mascarenhas Y (1986) Crystal structure analysis of deaminooxytocin: conformational flexibility and receptor binding. Science 232:633–636

Wüthrich K, Billeter M, Brown W (1983) Pseudo-structures for the 20 common amino acids for use in studies of protein conformations by measurements of intramolecular proton-proton distance constraints with nuclear magnetic resonance. J Mol Biol 169:949–961

Zhou GP, Troy FA (2003) Characterization by NMR and molecular modeling of the binding of polyisoprenols (PI) and polyisoprenyl recognition sequence (PIRS) peptides: three-dimensional structure of the complexes reveals sites of specific interactions. Glycobiology 13:51–57

Zhou GP, Troy FA (2005) NMR studies on how the binding complex of polyisoprenol recognition sequence peptides and polyisoprenols can modulate membrane structure. Curr Protein Pept 6:399–411